BMC Veterinary Research

RESEARCH

Open Access

# Morphological identification and distribution comparison of telocytes in pituitary gland between normal and cryptorchid yaks

Yumei Qi[1], Ligang Yuan[1*], Jianlin Zeng[1], Xiaofen Wang[1], Long Ma[1] and Jinghan Lv[1]

## Abstract

**Background** Telocytes (TCs) is a novel type of interstitial cells in many mammals organs, which participate in the organizational metabolism, mechanical support, immunomodulation and other aspects. The aim of this study was to explore the organizational chemical characteristics of TCs in pituitary gland and their changes in cryptorchid yaks.

**Methods** Transmission electron microscopy (TEM), toluidine blue staining, immunofluorescence, qRT-PCR, and Western blotting may enable us to understand TCs distribution characteristics and biological functions.

**Result** TEM confirmed the presence of TCs in the pituitary gland with small bodies and moniliform telopodes (Tps). The Tps extending out from the cell body to the peri-sinusoidal vessels spaces, the number of Tps is closely related to the morphology of the nucleus. The most obvious changes of TCs in the pituitary gland of cryptorchid yaks is the Tps are relatively shorter and decreased secretory vesicles. H.E. and toluidine blue staining revealed that TCs not only distributed between the sinusoidal blood vessels and the glandular cell clusters, but also present on the surface of vascular endothelial cells. The co-expression of TCs biomarkers, such as Vimentin/CD34, CD117/CD34 and α-SMA/CD34, were evaluated by immunofluorescence to further determine the phenotypic characteristics of TCs. Besides, we analyzed the mRNA and protein expression of these biomarkers to determine the characteristics of TCs changes and possible biological roles. Both the mRNA and protein expression of CD117 were significantly higher in the pituitary gland of cryptorchid yaks than in the normal ($p < 0.01$), the protein expression of CD34 in the cryptorchid yaks was significantly higher than the normal ($p < 0.01$). There were no significant difference in mRNA expression of Vimentin and α-SMA ($p > 0.05$), while the protein expression were significantly increased in the normal yaks ($p < 0.05$).

**Conclusions** In summary, this study reports for the first time that the biological characteristics of TCs in yak pituitary gland. Although there is no significant change in the distribution characteristics, the changes in biological features of TCs in cryptorchid yaks are clear, suggesting that TCs participated in alteration in the local microenvironment of the pituitary gland. Therefore, our study provides clues for further investigating the role of TCs in the pituitary gland during the occurrence of cryptorchidism in yaks.

**Keywords** Telocytes, Pituitary gland, Yaks, Cryptorchidism

*Correspondence:
Ligang Yuan
yuan2918@126.com
[1]College of Veterinary Medicine, Gansu Agricultural University, Lanzhou 730070, China

## Background

Telocytes (TCs) are a type of mesenchymal cells with small cell body and specific prolongations named telopodes (Tps), which formed by the interweaving of podomers and podoms, and the podoms contain endoplasmic reticulum, mitochondria, and caveolae [1]. Previous studies have shown that the Tps are very close to contact with blood vessels, nerve bundles, and local immune system cells through organ matrix distribution, forming a network between tissues, this network was considered to be the structural basis for cell communication [2, 3]. Furthermore, TCs establish unique spatial relationships with different cells to regulate the dynamic balance of the local microenvironment by contacting or releasing secretory vesicles [4, 5]. These secretory vesicles are considered to be "messengers" of substance exchange and signal transduction [6, 7]. TEM is the key detection methods to identify TCs [8]. Immunohistochemical staining are also applicable for identifying TCs because of the specific antigen markers for TCs. Currently, CD34 c-kit/CD117, Vimentin, and α-SMA are widely recognized as effective marker (immunological marker) of TCs and often combination with by double immunofluorescence staining [9].

More and more studies have demonstrated that TCs are present in different tissues of different species, such as pituitary gland [10], prostate [11], placenta [12], lungs [13], mammary glands [14], skeletal muscles [15], and so on. The pituitary gland, located on the ventral side of the hypothalamus, is a small oval-shaped body that is divided into the anterior (adenohypophysis) and the posterior pituitary (neurohypophysis).The pituitary gland secreting the corresponding gonadotropin which was stimulated by hypothalamic gonadotropin-releasing hormone to participate in maintaining the internal environment of the organism. Among them, the hypothalamic-pituitary-gonadal (HPG) axis is an important regulator of reproduction [16, 17]. The normal descent and postnatal development of mammalian testes are regulated by the reproductive endocrinology of hypothalamic-pituitary-testicular (HPT) axis. Liang et al. [10] demonstrated that the presence of TCs in the pars distalis pituitary gland of the rat and observed their ultrastructure, the TCs were tightly associated with the nerves in the peri-sinusoidal vessels spaces of the pituitary gland, implying that TCs might be related to nerve conduction. There are no relevant reports on TCs in pituitary gland, especially their roles in HPG [18]. Yaks are a unique bovine species endemic to high-altitude regions. Cryptorchidism is a common reproductive disorders and causing infertility in yaks. We reported for the first time TCs in testis and epididymis of yaks and further compared TCs in testis and epididymis of normal and cryptorchid yaks, which showed that Tps of cryptorchid yaks was significantly shorter than that of normal yaks, the surface labeling was also changed, and the TCs might be involved in the local substance metabolism [8]. Therefore, the present study were undertaken to provide insights into the biological characteristics of TCs in pituitary gland of yaks, and the possible function of TCs in cryptorchid yak. Our study will provide new clues for studying the mechanism of animal cryptorchidism.

## Results

### The TEM characteristics of TCs in pituitary gland between normal and cryptorchid yaks

TEM is the most effective method and considered to be the gold standard for determining TCs [19].TCs were observed in pituitary gland by TEM both in normal and cryptorchid yaks. TCs of pituitary gland in normal and cryptorchid yak are distributed in the interstitial spaces of glandular cells, near sinusoidal vessels, and on the surface of vascular endothelium (Fig. 1). The TCs in the interstitial spaces of the glandular cells were pear-shaped, with elongated Tps extending far away from the cell body with a large number of secretory vesicles. Compared with the normal group, the cell bodies of TCs in the cryptorchid group were small and the vesicles were significantly reduced (Fig. 1A-D). Nuclei of TCs near sinusoidal vessels were irregular. Nuclei of normal group TCs were triangular in shape, whereas nuclei of cryptorchid group TCs were pear-shaped, and Tps were shorter than in the normal group (Fig. 1E-H) [10]. Typical TCs were also seen on the surface of sinusoidal vessels with pear-shaped nuclei and elongated Tps with numerous secretory vesiclesc [20]. The Tps was longer in the normal group than in the cryptorchid group, and there were more secretory vesicles (Fig. 1I-L).

### Morphological model of TCs in pituitary gland

The morphological structure and the morphological model diagram of TCs in yak pituitary gland were proposed based on the results of TEM (Fig. 2).The TCs on the surface of vascellum and distribution in glandular cell clusters are pear shaped, with large nuclei and slender Tps, accompanied by numerous secretory vesicles. The nuclei of TCs near blood vessels is irregular, with multiple Tps of varying thickness closely connected to the vessels, which may be involved in material exchange and transportation.

### Optical microscopes

H.E results showed that the cells consisted of aidophilic cell (AC), basophilic cell (BC), and chromophobe cell (CC), distributed in clusters in pituitary gland. TCs were found in the capillary spaces of pituitary gland in normal and cryptorchid yaks, with small cell bodies and elongated protrusions (Fig. 3A-B). TCs were also distributed in the interstitial space between glandular cell clusters

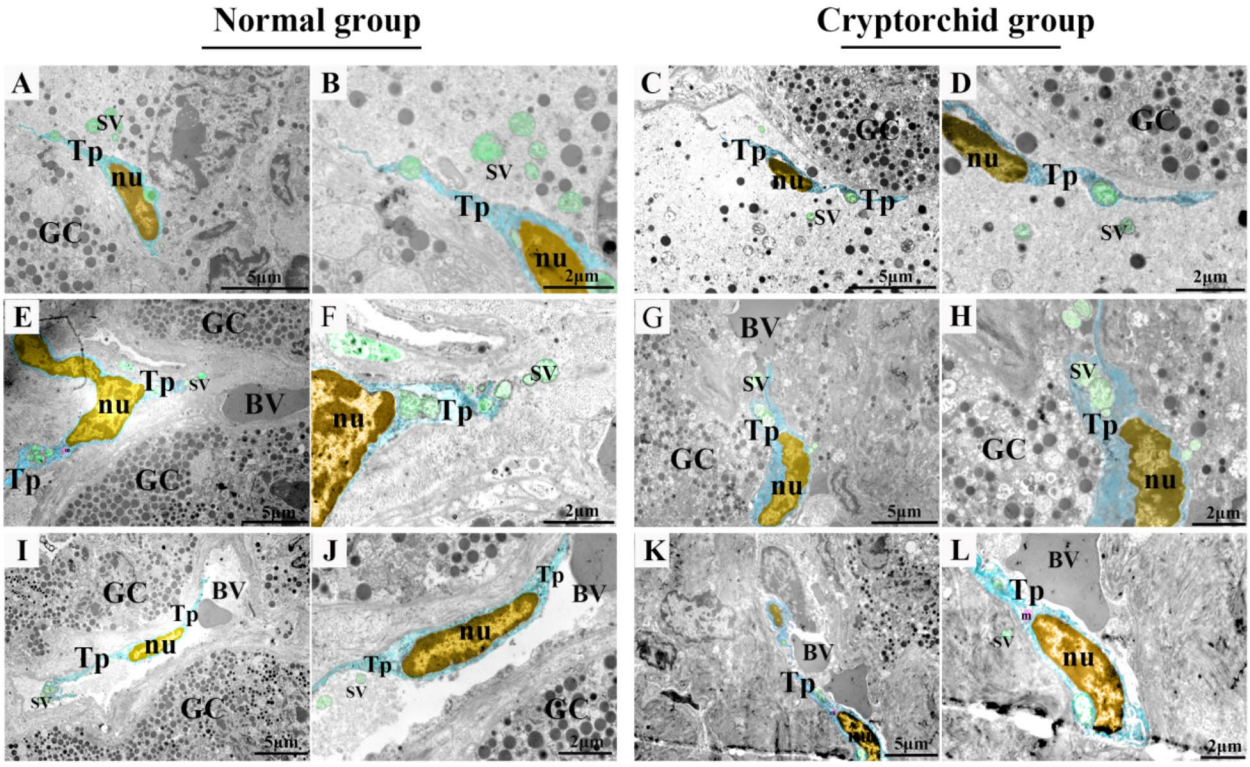


**Fig. 1** The localization of pituitary gland TCs in normal and cryptorchid yaks by TEM. (**A**–**D**) TCs distributed in the interstitial space of pituitary gland cells. Scale bars: 5 μm (**A**); 2 μm (**B**, **C**); 1 μm (**D**). (**E**–**H**) Distribution of TCs around sinusoidal capillaries in the pituitary gland of the yak. Scale bars: 5 μm (**G**); 2 μm (**E**, **F**, **H**). (**I**–**L**) TCs adhering to the endothelial surface of blood vessels. Scale bars: 5 μm (**I**, **J**, **K**); 1 μm (**J**). TCs were indicated with pseudo-color, Green color indicates extracellular vesicles. Tp: telopodes; nu: nucleus; BV: blood vessel; SV: secretory vesicles; m: mitochondria; GC: glandular cells. The pseudo-color TEM images were processed using Adobe Photoshop software (Adobe Systems, Inc., San Jose, CA, USA)

accompanied by secretory vesicles (Fig. 3C-D). In addition, TCs were also found in the endothelium of sinusoidal capillaries, which is consistent with the observation results of TEM (Fig. 3E-F).

Toluidine blue staining showed the strongly blue-labeled mesenchymal cells in the interstitial spaces of glandular cell clusters, around sinusoidal blood vessels, and the surface of capillary endothelial cells in pituitary gland of normal and cryptorchid yaks. The typical morphology of TCs is variously ellipsoidal, spindle and pear-shaped, with sparse cytoplasm and elongated protruding Tps (Fig. 4A–D).

#### Immunofluorescence analysis of TCs

Using double immunofluorescence, CD34/CD117 (Fig. 5A–C), CD34/vimentin (Fig. 5E–G), and CD34/α-SMA (Fig. 5I–K)double-positive cells which also presented with small cell bodies and extremely thin processes which extended far away from the cell body were detected in the pituitary gland of normal yak. Compared with the normal group, the pituitary gland TCs in the cryptorchidism group showed the same phenotypic characteristics, with co expression of CD34/CD117 (Fig. 5a–c), CD34/vimentin (Fig. 5e–g), and CD34/α - SMA (Fig. 5i–k).

#### The mRNA and protein expression of effective markers of telocytes in yak pituitary

The expression of *CD34*, *Vimentin*, *CD117*, and *α-SMA* mRNA in yak pituitary gland was detected by qRT-PCR. The expression of *CD117*mRNA was significantly higher in the pituitary gland of cryptorchid yaks than in the normal group, whereas the mRNA expression of *CD34*, *Vimentin* and *α-SMA* no difference in pituitary gland between normal and cryptorchid yaks ($p > 0.05$) (Fig. 6A).

Western blotting results showed that the relative expression of the proteins of CD34 and CD117 were significantly higher in the pituitary gland of cryptorchid yaks than in the normal ($p < 0.01$), whereas the expression of Vimentin and α-SMA was much higher in the pituitary gland of normal yaks than in the cryptorchidism ($p < 0.05$). In conclusion, the expression trends of the four proteins and their mRNA expression trends were basically the same (Fig. 6B-C).

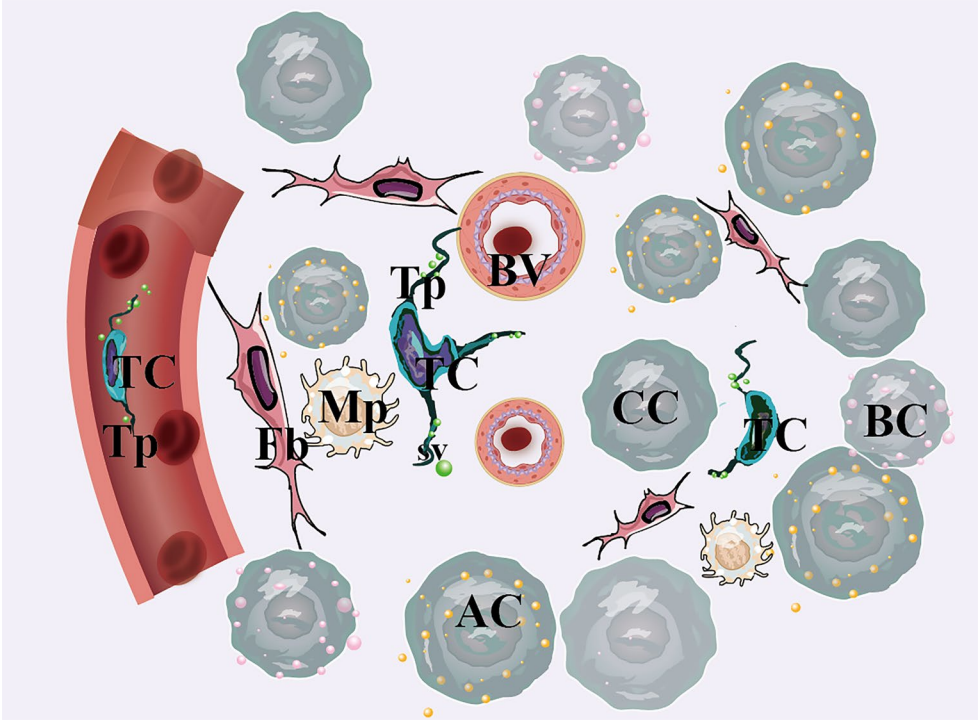


**Fig. 2** Model of TCs in the pituitary gland of the yak. Telocytes(TC), Acidophilic cell(AC), Basophiliccell(BC), chromophobecell(CC), Macrophage(Mp), Fibroblasts(Fb), blood vessel(BV), Secretory vesicle(SV). This image was drawn using Adobe Illustrator (2023 version)

## Discussion

TCs are widely distributed in vertebrate organelles. TCs can connect with both homogeneous (TCs with TCs) and heterogeneous (TCs with other types of cells) cells to form a complex three-dimensional (3D) network due to irregular cell bodies and elongated Tps, which play an important role in intercellular signaling. Studies have shown that TCs and Tps in the Pars distalis of the rat pituitary gland were closely connected to sinusoid vessels, glandular cells, extracellular vesicles and most crucially the nerves. Hence, TCs might be associated with neural-humoral dual regulation in the rat pituitary gland [10]. In this study, we found that the TCs were distributed in the adenocyte and peri-sinusoidal vessels space, and surface of vascular endothelial cells in pituitary gland of normal and cryptorchid yak. It was found that the morphology of the TCs cytosol often changed slightly with the change in the number of Tps [21]. The same conclusion was found in the present study, TCs around the perisinusoidal vessels of the pituitary gland were triangular in shape and found to be prolonged in three Tps, whereas spindle-shaped TCs have two Tps. Therefore, the number of Tps is closely related to the morphology of the TCs. In addition, compared with the normal yaks, the most obvious changes of TCs in the pituitary gland of cryptorchid yaks is the Tps are relatively shorter and decreased secretory vesicles. Therefore, it can be considered that the intercellular network of TCs is altered in the pituitary gland of cryptorchid yaks.

The TCs in the yak pituitary gland had small bodies with scarce cytoplasm, and also had extremely elongated Tps with numerous secretory vesicles. Previous studies have showed that secretory vesicles exist in TCs found in the human testis, myocardium, ovary, and other tissues. Considered the "messengers" of TCs that communicate with the outside world [7, 22], the TCs networks might interact with pituitary cell networks to participate in inter-glandular cell communication and long-distance signaling [10]. In our study, secretory vesicles distributed inside and outside Tps, which is one of the important features of TCs. Some studies have suggested that secretory vesicles were periodically generated in the interstitial space by TCs, these extracellular organelles seem to participate in sophisticated intercellular communication [23]. The reduction of secretion vesicles in the pituitary gland TCs of cryptorchid yaks may affect TCs network communication, and further analysis is needed to determine its potential impact on hormone feedback regulation in cryptorchidism.

Cytochemical characteristics are the main indicators to identify TCs from other mesenchymal cells. Consistent with the TME results, TCs can be observed in pituitary gland by use H.E and toluidine blue staining. It has typical cellular characteristics and is mainly distributed in the

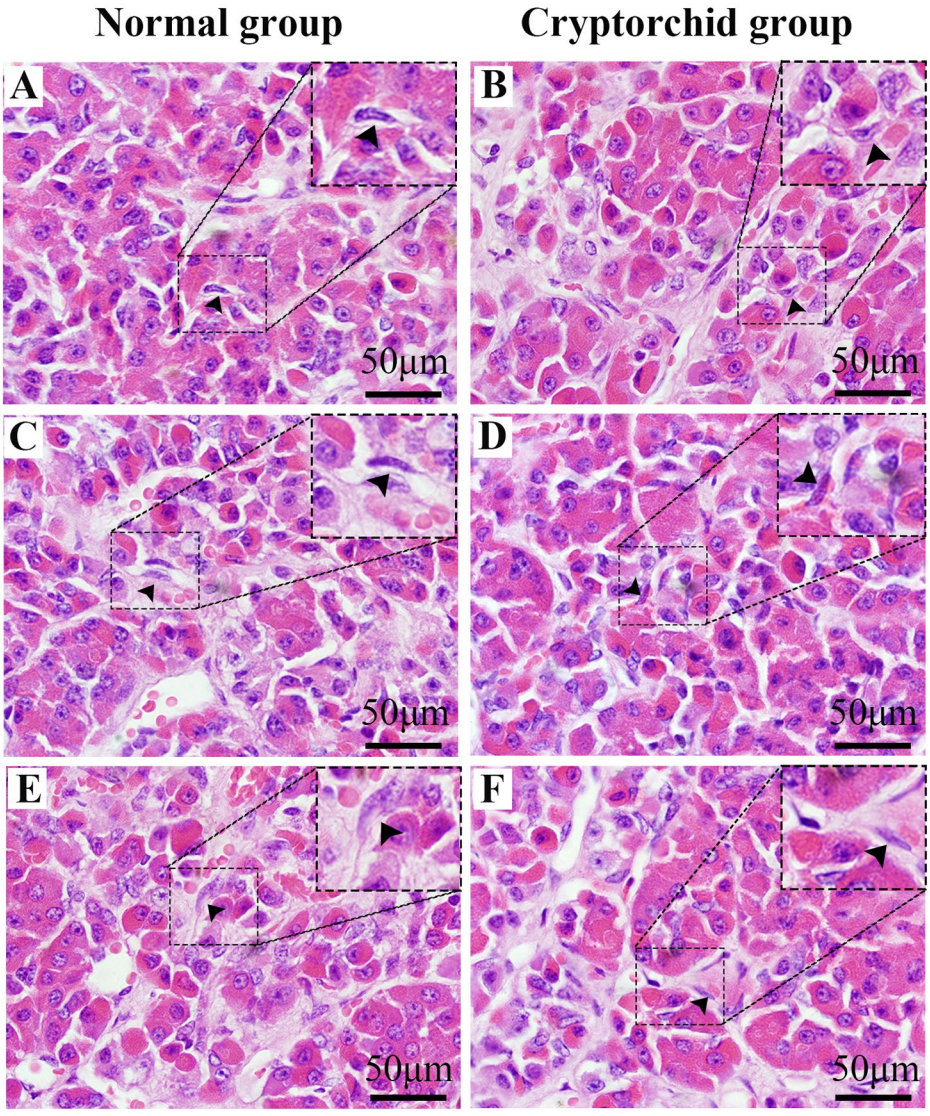


**Fig. 3** The H.E staining of pituitary gland in normal and cryptorchid yaks. (**A-B**) Distribution of interstitial cells in yak pituitary. (**C-D**) TCs adjacent to sinus vessels. (**E-F**) TCs on the surface of vascular endothelial cells. The black arrow indicates TCs, Scale bars: 50 μm

adenocyte and peri-sinusoidal vessels space, and surface of vascular endothelial cells.

The distribution of TCs in different organs is closely related to their functions. Research has shown that the fetal meninges were found to have more TCs than the adult, and hypothesized that the number of TCs may be related to meningeal stem cell activity [24, 25]. Our previous research has shown that the TCs distributed around the capillaries of yak epididymis may be associated with angiogenesis and material exchange [8]. Studies have found that TCs in camel epididymis were positive to vascular endothelial growth factor and can promot angiogenesis by secreting microRNA-containing extracellular vesicles [26, 27]. It has also been found that TCs distributed near equine tendon capillaries may contribute to the regulation of the vascular microecological environment [28]. In this study, TCs were distributed in the interstitial spaces of glandular cell clusters and had abundant vesicles, which may be involved in heterocellular communication regulated through gap connections and exosomes. Notably, we found that TCs were distributed on the surface of vascular endothelial cells of yak pituitary, which is consistent with Zhang's findings, this distribution pattern is considered to be related to maintain the smoothness and integrity of the vessel wall [20]. TCs perhaps participated in the process of neovascularization and repair through secreted factors and protein regulation [29]. An increasing body of evidence suggests that TCs may cooperate with tissue-resident stem cells to benefits the organ repair and regeneration, and that the damage

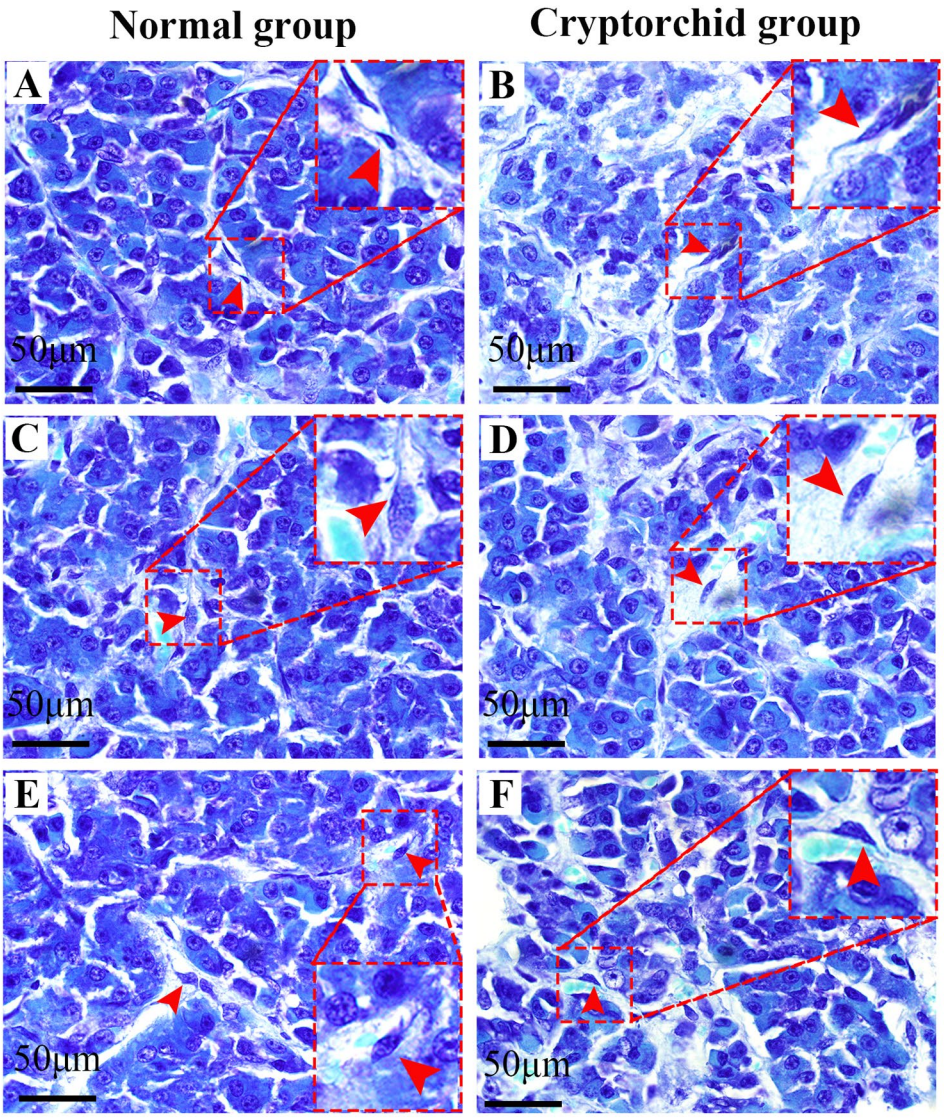


**Fig. 4** Results of toluidine blue staining in the pituitary gland of normal and cryptorchid yaks. (**A-B**) Distribution of interstitial cells in yak pituitary. (**C-D**) TCs adjacent to sinus vessels. (**E-F**) TCs on the surface of vascular endothelial cells. The red arrow indicates TCs, Scale bars: 50 μm

and dysfunction of TCs occurred during functional disorders [30]. Our research shows that the distribution of TCs in the pituitary gland of the normal and cryptorchid yaks is basically the same, suggesting that their functions are closely related to glandular cell secretion and vascular permeability, and further design is needed to verify changes in cellular chemical properties.

Since conducting research on TCs, there are several biomarkers of TCs have been reported, such as c-Kit/CD117, CD34, PDGFR-α, PDGFR-β, Vimentin, EGFR,α-SMA, connexin, caveolin and Sca-1 [31–34]. Numerous reports have detected TCs in different tissues display different phenotypes, e.g., rat pituitary gland TCs express vimentin and CD34, human testicular TCs express CD34 and PDGFRα [35]. We detected the CD34/vimentin, CD34/CD117, and CD34/α-SMA double-positive cells, which also presented with small cell bodies and extremely thin processes extended far away from the cell body, all of these double immunofluorescence reaction are combination with TEM features of the TCs in yaks pituitary gland.

To further analyze the role of TCs characteristics in yak cryptorchidism, we comparatively analyzed the expression of mRNAs and proteins of TCs surface markers in the pituitary gland between the normal and cryptorchid yak, both the mRNA and protein expression of CD117 were significantly higher in cryptorchid yaks than in the normal. The CD117 is a stem cell factor that is usually highly expressed in hematopoietic stem cells and tumor cells [31]. CD117 expression is restricted to a

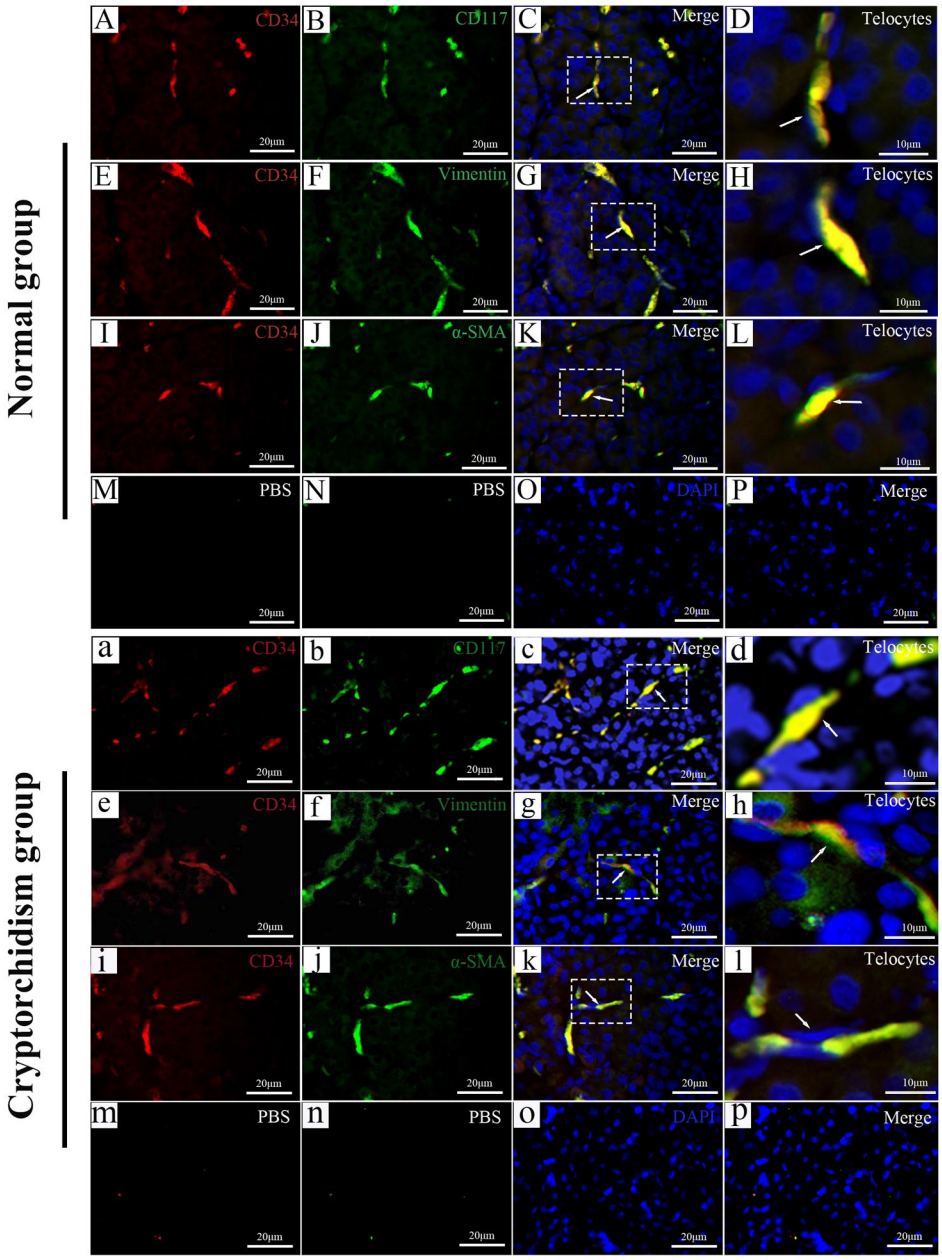


**Fig. 5** Double immunofluorescence results of normal and cryptorchid yaks pituitary gland staining for CD34/CD117, CD34/vimentin, and CD34/α-SMA. (**A–L**) Immunofluorescence results of TCs in normal yak pituitary gland. (**a–l**) Immunofluorescence results of TCs in cryptorchid yak pituitary gland. (**M–P**, **m–p**) Negative control group.The White arrow indicates TCs, Scale bar: 20 μm (**A–C**, **E–G**, **I–K**, **M–P**, **a–c**, **e–g**, **i–k**, **m–p**), Scale bar: 10 μm (**D**, **H**, **L**, **d**, **h**, **l**)

relatively small number of cell types, suggesting a tendency towards carcinoma [33]. Studies have suggested that the occurrence of cryptorchidism may be accompanied by a risk of cancer in undescended testicles [36]. Therefore, the high expression of CD117 in the pituitary gland of cryptorchid yaks may serve as an early warning lights on gonadal lesions of HPG. CD34 is a marker receptor found on the surface of mesenchymal stem cells; it is also a highly glycosylated type I transmembrane glycoprotein expressed on the surface of hematopoietic stem/progenitor cells of humans and other mammals [37]. Numerous studies have found that $CD34^+$ cells may improve angiogenesis and tissue regeneration [38]. In this study, the high expression of CD34 in the pituitary gland of cryptorchid yaks may be related to a compensatory increase in vascularity and associated with local microcirculatory regulation. Vimentin, an abundant cytoplasmic intermediate filament protein, is recognized for its important role in stabilizing intracellular structure and vascular elasticity [39]. The α-SMA was shown to be the

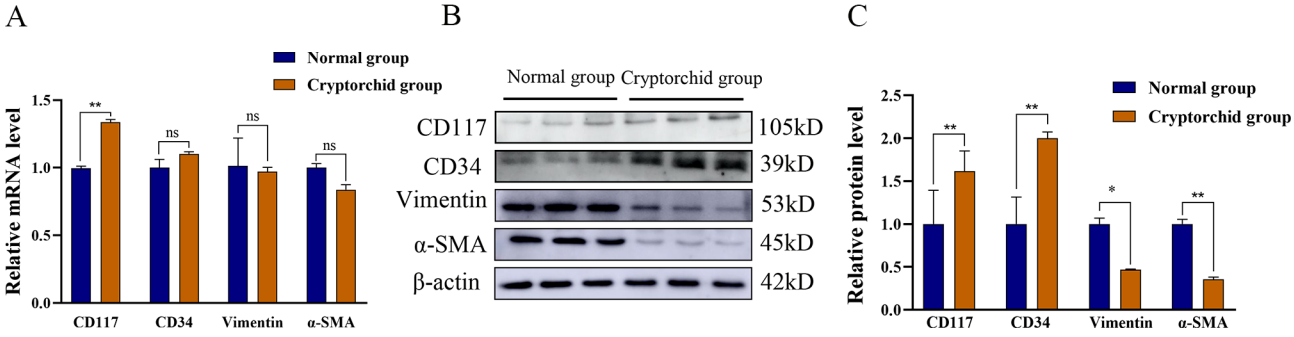


**Fig. 6** mRNA and protein expression of effective telocyte markers (CD117, CD34, vimentin, and α-SMA) in the pituitary gland of yak. (**A**) Relative mRNA expression levels. (**B**) Western blotting. (**C**) Relative protein expression levels. Each sample was tested three times. Results are expressed as the mean ± standard deviation, with β-actin gene and protein expression used as an internal control. ** $p < 0.01$, NS (not significant), $p > 0.05$

decisive cytoskeleton of the mechanical and elastic properties of Vascular smooth muscle cells [40]. In this study, the expression of vimentin and α-SMA in cryptorchid yaks was significantly lower than normal group, combining the close relationship between TCs distribution and blood vessels, the potential involvement of TCs in pituitary gland pathological changes and future possibilities of TCs may exert paracrine functions being able to reflect the predicted the impaired feedback/negative feedback of the HPT axis in the occurrence of cryptorchidism.

## Conclusion

This study reports for the first time that the biological characteristics of TCs in pituitary gland of normal and cryptorchid yaks. The most obvious changes of TCs in the pituitary gland of cryptorchid yaks is the Tps are relatively shorter and decreased secretory vesicles. In addition, the changes in biological features of TCs in cryptorchid yaks are clear, suggesting that TCs participated in alteration of the local microenvironment in the pituitary gland. Therefore, the future possibilities for targeting TCs as a novel therapeutic strategy to cryptorchidism and other reproductive diseases are worth attention.

## Materials and methods

### Animals and sample acquisition

The pituitary gland of normal yaks ($n=3$) and pituitary gland of cryptorchid yaks samples (a testicle not descending to the scrotum is judged as cryptorchidism, $n=3$) were collected from the designated slaughterhouse in Xining City, Qinghai Province. A portion of each sample was quickly frozen in liquid nitrogen, transported to the laboratory and then stored at −80 °C for RNA and protein extraction, the remaining samples were stored in 4% paraformaldehyde and 2.5% glutaraldehyde separately for histological and ultrastructural study. All experimental animals were approved by the Animal Care and Use Committee of the College of Veterinary Medicine, Gansu Agricultural University, and all experimental methods were performed according to relevant guidelines and regulations.

### Drugs and reagents

All experimental antibodies were purchased from commercial suppliers. Mouse Monoclonal antibody CD34 (bsm-41196 M), Rabbit polyclonal antibody vimentin (bs-8533R), CD117 (bs-1005R) and β-actin(bs−0061R) were purchased from Beijing BIOSS Antibodies Co., Ltd, China. Rabbit polyclonal antibody α-SMA(AF1032) were purchased from Affinity Biosciences Cat, China. Horseradish peroxidase-labeled goat anti-rabbit IgG H&L (SA00001–2) and Horseradish peroxidase-labeled goat anti- mouse IgG H&L (SA00001–1) were provided by Wuhan Proteintech Biotechnology Co., Ltd, China. Goat anti-Mouse IgG H&L (ab150115, Alexa Fluor® 647) and Goat anti-Rabbit IgG H&L (ab150077, Alexa Fluor® 488) were provided by Abcam, Cambridge, UK. ECL Plus ultrasensitive luminescent solution (PE0010) was purchased from Solebao Biotechnology Co., Ltd.

### TEM

The pituitary gland tissue of yak fixed in 2.5% glutaraldehyde was cut into small pieces (0.2 cm × 0.2 cm × 0.2 cm) and fixed in 2% osmium tetraoxide at 4 °C for 3 h. The pieces were dehydrated with a gradient acetone series (30%, 50%, 70%, 80%, 90%, 95%, and 100%) and then embedded in epoxy resin. Ultrathin sections were prepared and affixed to the copper mesh, stained with uranium acetate and lead citrate, and then examined using a JEM-100CX electron microscope (Japan NEC).

### Optical microscope

Fresh pituitary gland samples (0.5×0.5×0.5 cm) were fixed with 4% paraformaldehyde solution and rinsed in running water for 24 h before gradient ethanol dehydration(50%, 70%, 80%, 95%, 95%, and 100%). Subsequently, samples were made transparent with xylene(50% ethanol: 50% xylene, xylene), embedded using an Epon 812 paraffin embedding machine and sectioned at a thickness

of 4 μm using an ultramicrotome (Leica RM2235, Germany). Then, the paraffin sections were immersed in xylene, 100%, 90%, 80% and 70% (v/v) for 5 min, respectively, and washed with tap water for 5 min. Stained with H.E and toluidine blue, respectively, and finally neutral gum was used for sealing. Images were taken using an Olympus light microscope (DP73, Olympus, Tokyo, Japan).

#### Immunofluorescence

The deparaffinized sections were boiled in 10 mM sodium citrate buffer (pH 6.0) for antigen retrieval. Peroxidase activity was blocked by incubating the tissue sections with 3.0% hydrogen peroxide ($H_2O_2$) for 15 min at 37 ℃ and then blocked with blocking solution for 15 min. Then, the samples were incubated overnight at 4 °C with primary antibodies. The following primary antibodies were used for IF analysis: mouse polyclonal anti-CD34 (1:300), Rabbit polyclonal anti-Vimentin (1:300), CD117 (1:350), and α-SMA (1:300). After washing with 0.1 M PBS (pH 7.4), sections were incubated with the following fluorescent secondary antibodies for 1 h at 37 °C: Anti-Mouse IgG H&L AF647 (1:800) and Anti-Rabbit IgG H&L AF488 (1:800). Nuclei were routinely counterstained with DAPI. Finally, the sections were sealed with anti-fluorescence quencher. The negative control was incubated with PBS instead of primary antibody, with subsequent steps performed as described. Photographs were taken under a camera (DP73, Olympus, Tokyo, Japan).

#### Real-time quantitative polymerase chain reaction

Total RNA was extracted from yak pituitary gland tissues using TRIzol (Solarbio, Beijing, China) and immediately reverse transcribed using Prime Script RT kit with gDNA eraser (TransGen Biotech, Beijing, China). Primer Premier 5.0 software was used (Primer Biosoft International, Palo Alto, USA) was used to design primers; the primer sequence was obtained with reference to the NCBI database (www.ncbi.nlm.nih.gov), and the primer information is shown in Table 1. qRT-PCR was performed using a Light Cycler 480 thermocycler (Roche, Mannheim, Germany) in a final reaction volume of 20 μL, comprising 1 μL of cDNA, 1 μL of forward primer, 1 μL of reverse primer, 10 μL of 2×SYBR Green II PCR mix (TransGen Biotech, Beijing, China), 0.4 μL of ROX reference dye, and 6.6 μL of nuclease-free $H_2O$. The cycling reaction conditions were 95 °C for 30 s; followed by 95 °C, for 5 s, and 60 °C for 30 s each, for a total of 45 cycles. Three replicates were performed for each sample to ensure relative expression accuracy of the target genes. β-Actin was used as a reference gene. The relative expression of target genes was calculated using the $2^{-\Delta\Delta CT}$ method.

#### Western blot

Pituitary gland tissue samples were lysed using a radioimmunoprecipitation assay buffer (Solarbio) containing 1:100 (v/v) phenylmethylsulfonyl fluoride (Solarbio) and were then centrifuged at 12,000 rpm for 5 min at 4 ℃to obtain protein samples. Protein was mixed with 4 × loading buffer (Solarbio) and separated using 10% sodium dodecyl sulfate-polyacrylamide gel electrophoresis. The separated proteins were then transferred onto polyvinylidene fluoride membranes (Millipore, Atlanta, GA, USA) and washed with Tris-buffered saline with Tween 20 (TBST; Solarbio) at room temperature for 30 min. The membranes were blocked with 5% skim milk in TBST at room temperature for 30 min and incubated with antibodies against CD34 (1:500), CD117(1:500), Vimentin(1:500), and α-SMA(1:500) at 4 °C for 8 h, with β-actin (1:3000) as an internal reference. The membranes were then washed and incubated with HRP-conjugated AffiniPure goat anti-rabbit IgG H&L (1:4000) or HRP-conjugated AffiniPure goat anti-mouse IgG H&L (1:4000). The membranes were exposed to the ECL Plus chemiluminescence western blotting detection solution and the signal detected with Amersham Imager 600 (GeneralElectric Company, USA). And the signal was quantified using ImageJ 10.0 software (National Institute of Health, Bethesda, MD, USA).

**Table 1** List of the primers information

| Gene | Sequences(5′→3′) | Product length(bp) | Tm(℃) | Accession no. |
|---|---|---|---|---|
| *CD117* | AATGTGAAGCGCGAGTACCA | 165 | 58 | XM_061420190.1 |
| | ACACAGACACAACTGGCACA | | | |
| *CD34* | AGGCCATTGTGAATCGAGGG | 101 | 58 | XM_014483307.1 |
| | CAGTTCGGTATCAGCCACCA | | | |
| *Vimentin* | ACCAGCTCACCAACGACAAA | 168 | 60 | XM_005891917.2 |
| | GACGTGCCAAAGAGGCATTG | | | |
| *α-SMA* | CGTTCAGCCCCAAGATAACG | 178 | 60 | XM_005897715.2 |
| | GCTGTGCTATGAACGTGTGC | | | |
| *β-actin* | ATCATTGCTCCCCCAGAACG | 160 | 60 | XM_005897464.1 |
| | TAGCATGGAAGCCCAGTCAG | | | |

### Statistical analysis

Statistical analyses were performed using SPSS 21.0 (IBM Corporation, Armonk, NY, USA). Quantitative data are presented as the mean ± standard deviation of the mean. All data were tested for normality and homoscedasticity and subjected to one-way analysis of variance followed by Duncan's multiple range test. Differences at $p < 0.05$ were considered to be statistically significant.

#### Abbreviations

| | |
|---|---|
| TCs | Telocytes |
| TEM | Transmission electron microscopy |
| Tps | Telopodes |
| nu | Nucleus |
| SV | Secretory vesicles |
| BV | Blood vessel |
| m | Mitochondria |
| GC | Glandular cells |
| AC | Acidophilic cell |
| BC | Basophiliccell |
| CC | Chromophobecell |
| Mp | Macrophage |
| Fb | Fibroblasts |
| BV | Blood vessel |
| 3D | Three-dimensional |

## Supplementary Information

The online version contains supplementary material available at https://doi.org/10.1186/s12917-024-04307-1.

Supplementary Material 1

#### Acknowledgements

We thank Institute of Animal Husbandry and Veterinary Medicine, Chinese Academy of Agricultural Sciences for helping TEM measurements. We thank all the colleagues who assisted in this study.

#### Author contributions

Q.Y.: Conceptualization, Data curation, Formal analysis, Methodology, Writing - original draft. Y.L.: Conceptualization, Funding acquisition, Writing - review & editing. Z.J. and W.X.: Validation, Visualization. M.L. and L.J.: Data curation. All authors have read and approved the final version of the manuscript.

#### Funding

This study supported by the Natural Science Foundation of Gansu Province, China (Grant No. 23JRRA1420), National Nature Science Foundation of China (Grant No. 31160488) and The fund of Animal Clinical Practice Project of Gansu Agricultural University (NO. GSAU-JSFW-2023-07; NO. GSAU-JSFW-2023-08).

#### Data availability

The datasets obtained and/or analyzed during the current study are available from the corresponding author upon reasonable request.

## Declarations

#### Ethics approval and consent to participate

All experimental animals were approved by the Animal Care and Use Committee of the Veterinary College of Gansu Agricultural University (Ratification number: GSAU-Eth-VMC-2021-010), and all methods were performed in accordance with the relevant guidelines and regulations.

#### Consent for publication

Not applicable.

#### Competing interests

The authors declare no competing interests.

Received: 9 August 2024 / Accepted: 30 September 2024
Published online: 11 October 2024

#### References

1. Vannucchi MG. The telocytes: ten years after their introduction in the scientific literature. An update on their morphology, distribution, and potential roles in the gut. Int J Mol Sci. 2020;21(12).
2. Varga I, Danisovic L, Kyselovic J, Gazova A, Musil P, Miko M, Polak S. The functional morphology and role of cardiac telocytes in myocardium regeneration. Can J Physiol Pharmacol. 2016;94(11):1117–21.
3. Zheng Y, Zhang M, Qian M, Wang L, Cismasiu VB, Bai C, Popescu LM, Wang X. Genetic comparison of mouse lung telocytes with mesenchymal stem cells and fibroblasts. J Cell Mol Med. 2013;17(4):567–77.
4. Faussone Pellegrini MS, Popescu LM. Telocytes Biomol Concepts. 2011;2(6):481–9.
5. Kondo A, Kaestner KH. Emerging diverse roles of telocytes. Development. 2019;146(14).
6. Manole CG, Cismaşiu V, Gherghiceanu M, Popescu LM. Experimental acute myocardial infarction: telocytes involvement in neo-angiogenesis. J Cell Mol Med. 2011;15(11):2284–96.
7. Nicolescu MI, Popescu LM. Telocytes in the interstitium of human exocrine pancreas: ultrastructural evidence. Pancreas. 2012;41(6):949–56.
8. Yang D, Yuan L, Chen S, Zhang Y, Ma X, Xing Y, Song J. Morphological and histochemical identification of telocytes in adult yak epididymis. Sci Rep. 2023;13(1):5295.
9. Rosa I, Marini M, Manetti M. Telocytes: an emerging component of Stem Cell Niche Microenvironment. J Histochem Cytochem. 2021;69(12):795–818.
10. Chunhua L, Xuebing B, Yonghong S, Min Y, Haixiang H, Jianming Y, Zhenwei Z, Qiusheng C. Distribution and Ultrastructural Features of Telocytes in the pars distalis of the rat pituitary gland. Microsc Microanal. 2023;29(2):658–64.
11. Felisbino SL, Sanches BDA, Delella FK, Scarano WR, Dos Santos FCA, Vilamaior PSL, Taboga SR, Justulin LA. Prostate telocytes change their phenotype in response to castration or testosterone replacement. Sci Rep. 2019;9(1):3761.
12. Bosco C, Díaz E. Presence of telocytes in a non-innervated organ: the Placenta. Adv Exp Med Biol. 2016;913:149–61.
13. Tang L, Song D, Qi R, Zhu B, Wang X. Roles of pulmonary telocytes in airway epithelia to benefit experimental acute lung injury through production of telocyte-driven mediators and exosomes. Cell Biol Toxicol. 2023;39(2):451–65.
14. Popescu LM, Andrei F, Hinescu ME. Snapshots of mammary gland interstitial cells: methylene-blue vital staining and c-kit immunopositivity. J Cell Mol Med. 2005;9(2):476–7.
15. Ravalli S, Federico C, Lauretta G, Saccone S, Pricoco E, Roggio F, Di Rosa M, Maugeri G, Musumeci G. Morphological Evidence of Telocytes in Skeletal Muscle Interstitium of Exercised and Sedentary Rodents. Biomedicines. 2021;9(7).
16. Alatzoglou KS, Gregory LC, Dattani MT. Development of the Pituitary Gland. Compr Physiol. 2020;10(2):389–413.
17. Zhang S, Cui Y, Ma X, Yong J, Yan L, Yang M, Ren J, Tang F, Wen L, Qiao J. Single-cell transcriptomics identifies divergent developmental lineage trajectories during human pituitary development. Nat Commun. 2020;11(1):5275.
18. Kuiri-Hänninen T, Koskenniemi J, Dunkel L, Toppari J, Sankilampi U. Postnatal testicular activity in healthy boys and boys with Cryptorchidism. Front Endocrinol. 2019;10:489.
19. Xuebing B, Ruizhi W, Yue Z, Chunhua L, Yonghong S, Yingxin Z, Baitao D, Tarique I, Ping Y, Qiusheng C. Tissue micro-channels formed by Collagen Fibers and their Internal Components: Cellular evidence of proposed Meridian conduits in Vertebrate skin. Microsc Microanal.2020;26(5):1069–75.
20. Zhang H. Vascular telocytes. In: Telocytes Edn. 2016;913:377–95.
21. Lu S, Li H, Zhang H, Ge J. Research update on the association between telocytes distribution with blood vessels on various tissues and the biological properties of telocytes. Zhonghua Xin xue guan bing za zhi. 2014;42(4):352–6.
22. Sanches BDA, Tamarindo GH, Maldarine JDS, Da Silva ADT, Dos Santos VA, Góes RM, Taboga SR, Carvalho HF. Telocytes of the male urogenital system: interrelationships, possible functions, and pathological implications. Cell Biol Int. 2021;45(8):1613–23.
23. Popescu LM, Gherghiceanu M, Suciu LC, Manole CG, Hinescu ME. Telocytes and putative stem cells in the lungs: electron microscopy, electron tomography and laser scanning microscopy. Cell Tissue Res. 2011;345(3):391–403.

24. Siegenthaler JA, Pleasure SJ. We have got you 'covered': how the meninges control brain development. Curr Opin Genet Dev. 2011;21(3):249–55.
25. Nakagomi T, Molnár Z, Nakano-Doi A, Taguchi A, Saino O, Kubo S, Clausen M, Yoshikawa H, Nakagomi N, Matsuyama T. Ischemia-induced neural stem/progenitor cells in the pia mater following cortical infarction. Stem Cells Dev. 2011;20(12):2037–51.
26. Hussein MT, Abdel-Maksoud FM. Structural investigation of Epididymal Microvasculature and its relation to Telocytes and Immune cells in Camel. Microscopy Microanalysis: Official J Microscopy Soc Am Microbeam Anal Soc Microscopical Soc Can. 2020;26(5):1024–34.
27. Cismaşiu VB, Popescu LM. Telocytes transfer extracellular vesicles loaded with microRNAs to stem cells. J Cell Mol Med. 2015;19(2):351–8.
28. Luesma MJ, Cantarero I, Sánchez-Cano AI, Rodellar C, Junquera C. Ultrastructural evidence for telocytes in equine tendon. J Anat. 2021;238(3):527–35.
29. Zhao B, Liao Z, Chen S, Yuan Z, Yilin C, Lee KK, Qi X, Shen X, Zheng X, Quinn T, et al. Intramyocardial transplantation of cardiac telocytes decreases myocardial infarction and improves post-infarcted cardiac function in rats. J Cell Mol Med. 2014;18(5):780–9.
30. Ibba-Manneschi L, Rosa I, Manetti M. Telocyte implications in human pathology: an overview. Semin Cell Dev Biol. 2016;55:62–9.
31. Chang Y, Li C, Lu Z, Li H, Guo Z. Multiple immunophenotypes of cardiac telocytes. Exp Cell Res. 2015;338(2):239–44.
32. Hinescu ME, Gherghiceanu M, Mandache E, Ciontea SM, Popescu LM. Interstitial cajal-like cells (ICLC) in atrial myocardium: ultrastructural and immunohistochemical characterization. J Cell Mol Med. 2006;10(1):243–57.
33. Hostiuc S, Marinescu M, Costescu M, Aluaş M, Negoi I. Cardiac telocytes. From basic science to cardiac diseases. II. Acute myocardial infarction. Annals Anat = Anatomischer Anzeiger: Official Organ Anatomische Gesellschaft. 2018;218:18–27.
34. Suciu L, Popescu LM, Gherghiceanu M, Regalia T, Nicolescu MI, Hinescu ME, Faussone-Pellegrini MS. Telocytes in human term placenta: morphology and phenotype. Cells, tissues, organs. 2010;192(5):325–39.
35. Marini M, Rosa I, Guasti D, Gacci M, Sgambati E, Ibba-Manneschi L, Manetti M. Reappraising the microscopic anatomy of human testis: identification of telocyte networks in the peritubular and intertubular stromal space. Sci Rep. 2018;8(1):14780.
36. Wood HM, Elder JS. Cryptorchidism and testicular cancer: separating fact from fiction. J Urol. 2009;181(2):452–61.
37. Hua P, Roy N, de la Fuente J, Wang G, Thongjuea S, Clark K, Roy A, Psaila B, Ashley N, Harrington Y, et al. Single-cell analysis of bone marrow-derived CD34 + cells from children with sickle cell disease and thalassemia. Blood. 2019;134(23):2111–5.
38. Hassanpour M, Salybekov AA, Kobayashi S, Asahara T. CD34 positive cells as endothelial progenitor cells in biology and medicine. Front cell Dev Biology. 2023;11:1128134.
39. Paulin D, Lilienbaum A, Kardjian S, Agbulut O, Li Z. Vimentin: regulation and pathogenesis. Biochimie. 2022;197:96–112.
40. Zhu Y, Qu J, He L, Zhang F, Zhou Z, Yang S, Zhou Y. Calcium in vascular smooth muscle cell elasticity and adhesion: Novel insights into the mechanism of action. Front Physiol. 2019;10:852.


## Publisher's note